Rapid changes in track, intensity, and structure at landfall

Marie-Dominique Leroux, Kim Wood

WMO/CAS/WWW

FOURTH INTERNATIONAL WORKSHOP ON TROPICAL CYCLONE LANDFALL PROCESSES

Rapid changes in track, intensity, and structure at landfall

Chair: Marie-Dominique Leroux
Cellule Recherche Cyclones, Météo-France
Direction Interrégionale pour l'Océan Indien
50 boulevard du Chaudron, 97490 Sainte-Clotilde

Rapporteur: Kim Wood
Department of Geosciences, Mississippi State University
108 Hilbun Hall, 355 Lee Blvd., Mississippi State, MS, USA

Working Group Members: Nancy Baker (NRL-Monterey), Esperanza Cayanan (PAGASA), Difei Deng (UNSW-Canberra and IAP), Russ Elsberry (Naval Postgraduate School), Eric Hendricks (Naval Postgraduate School), Matt Kucas (JTWC), Jia Liang (Nanjing University of Information Science and Technology), Kuo-Chen Lu (Taiwan Central Weather Bureau), Peter Otto (BoM), Nanan Qin (Nanjing University of Information Science and Technology), Buck Sampson (NRL-Monterey), Hsiao-Chung Tsai (Tamkang University), Liguang Wu (Nanjing University of Information Science and Technology), Zifeng Yu (Shanghai Typhoon Institute/CMA)

Abstract

This report summarizes the current state of research on rapid changes in tropical cyclone (TC) track, intensity, and structure at landfall. It also details advances in operational practices regarding forecasts and warnings of these systems as they approach land. Current and ongoing challenges are addressed as well. The report concludes with recommendations and requests from both researchers and forecasters regarding future directions.

1. Introduction

Accurate forecasts of the timing, location, and impacts of tropical cyclone (TC) landfall remain an ongoing challenge. A recent example is Cyclone Debbie (2017), which rapidly intensified prior to landfall in Queensland, Australia. Debbie caused an estimated USD $1.85 billion in damage and 14 fatalities, making it the deadliest Australian cyclone since Cyclone Tracy in 1974 (Davidson 2017, personal comm.). Not only did Debbie rapidly intensify, it also shifted direction before it hit land, impacting locations that had not been advised to evacuate. Environmental factors such as weak steering flow and changes in vertical wind shear contributed to the forecast challenges associated with Cyclone Debbie.

This case demonstrates the ongoing need to improve our understanding and prediction of rapid intensification, particularly for TCs near coastlines. In addition, properly characterizing the near-coastal atmospheric environment can be crucial for TC track and structural changes prior to landfall and as the TC makes landfall. Structural changes subsequently affect the distribution of hazardous winds and rainfall, the latter of which can extend far inland.

While it is important to accurately analyze position, intensity and structure as the first step in the forecasting process for any TC, the analysis is particularly crucial for TCs nearing landfall since trends in these characteristics tend to persist in the short-term. For positioning, scatterometer and microwave sensor imagery from low earth-orbiting satellite have consistently provided essential depictions of TC convective structure, including center features that influence forecasters' TC best track adjustments.

Frequent aircraft reconnaissance missions sampling both the storm and the near-storm environment provided invaluable data to National Hurricane Center (NHC) forecasters as Hurricane Harvey (2017) bore down on Texas and Hurricane Irma (2017) approached Florida. Though the Advanced Baseline Imager (ABI; Schmit et al. 2017) on GOES-16 was not operational during the hyperactive 2017 Atlantic hurricane season and its data were preliminary, these higher spatial and temporal resolution observations provided additional, invaluable information to forecasters and researchers. A similar instrument on the Himawari-8 geostationary satellite operated by the Japan Meteorological Agency has provided multi-channel, high resolution imagery since it became operational in 2015. These data have improved forecasters' ability to monitor and track TCs in the western Pacific Ocean.

However, not all TC basins have sufficient resources to provide adequate warnings and risk mitigation strategies. In the southwest Indian Ocean (SWIO), Leroux et al. (2017) showed that Madagascar, the fourth largest island on earth and one of the poorest countries in the world, was threatened (hit) twice (once) a year by tropical systems and once every two (four) years by TCs, mostly on its eastern coast. Mozambique, another poor country located on the eastern coast of Africa between Tanzania and South Africa, was hit by tropical systems once a year on average and by TCs about once every three years from the 1999/2000 to 2015/16 seasons.

Despite the frequency of TC-related impacts in the Philippines (an average of 20 per year), operational TC forecasting remains a challenge for Filipino forecasters, especially when a TC undergoes rapid changes in intensity and/or moves erratically near the coast. During 2014-2016, 48 TCs impacted the region, and forecast error associated with these systems was consistently higher for recurving TCs of lower intensities (Table 1). Though recurvature forecasts depend on understanding the synoptic-scale environmental flow, which tends to be well predicted, the timing and degree of recurvature can be difficult to predict accurately, particularly for rapid changes in direction.

INTENSITY	FORECAST ERROR (km)		
	24-hr	48-hr	72-hr
RECURVING TC			
Tropical Storm	169.52	301.33	492.46
Typhoon	106.69	149.06	166.18
NONRECURVING TC			
Tropical Storm	142.69	261.08	410.12
Typhoon	86.96	145.77	223.57

***Table 1**. Average forecast track error of recurving and non-recurving TCs in the Philippines from 2014-2016.*

As the concentration of people and industry increases in coastal regions, the requirement for extended lead times for TC landfall forecasts and warnings becomes increasingly important. A capability for 7-day (or even longer) track forecasts by deterministic and by ensemble numerical weather

prediction (NWP) models has been demonstrated by NWP centers in several countries. In general, the capability for TC intensity forecasts is much more limited. Global NWP models do not have the horizontal grid resolution to resolve the inner-core vortex structure (and physical processes), and at best provide intensity trend forecasts. Regional NWP models have both the grid resolution and the physical process parameterization to better predict the TC intensity, but the regional model intensity guidance tends to be degraded after 3 days – in part due to degraded TC track forecast accuracy. Thus, while 7-day track forecast guidance is available, an extended lead time and improved accuracy of intensity forecast guidance is required.

This report discusses recent (2014-present) research and updates to operational practices within the following sections: analog approaches to forecasting, recent advances in TC observing systems, track changes, numerical investigations of TCs near land, intensity change (particularly rapid intensity change), TC structural evolution near land, and operational approaches and challenges.

2. Analog approaches to forecasting

Analog approaches employ past TCs with similar characteristics to current events to develop forecasts based on those similarities. For example, if an historical TC near Taiwan exhibited similar structure to a currently active storm, it may highlight mesoscale phenomena caused by terrain effects that could impact the track of the current event (Huang et al. 2016).

Recently, these analog approaches have been applied to intensity forecasting. Tsai and Elsberry (2014) developed a 5-day Weighted Analog Intensity technique for WNP TCs (WAIP) using cases with similar tracks and initial intensities to the target TC. They hypothesized the track was a primary determinant of intensity change in the 3-5 day time frame, thus analogs (past TCs) which best match the 3-5 day tracks are weighted higher. This simple analog technique demonstrated greater accuracy than regional numerical model guidance in 3-5 day forecasts, and it can be calculated in a few minutes on a desktop computer (Tsai and Elsberry 2016).

However, independent testing revealed an increasingly large intensity over-forecast bias in the 5-7 day interval that Tsai and Elsberry (2015) attributed to “ending storms” due to landfall, extratropical transition, or delayed development. As a result, Tsai and Elsberry (2017) developed an “ending storm” version of the 7-day WAIP, modified to separately forecast ending and non-ending storms within the 7-day forecast interval. The ending storm constraint of only selecting analogs with intensities < 50 kt is particularly effective if the TC is known to end in the 4- to 7-day forecast interval (Fig. 1). By contrast, this independent set of ending storms has much larger MAEs if the All Sample (including both ending and non-ending storms) bias correction is utilized, because, rather than leveling off after 84 h, the MAEs continue to increase to ~23 kt at 144 and 156 h (Fig. 1a).

A separate calibration of the intensity spreads was developed for the training set to ensure that 68% of the verifying intensities will be within the 12-h WAIP intensity spread values results (Fig. 1c, Tsai and Elsberry 2017). Because progressively smaller numbers of storms are extending to 156 h before ending, the mean intensity spreads become smaller with increasing forecast interval (and thus are under-dispersive). After the calibration of the intensity spreads, the mean intensity spreads are made smaller from 12 h to 24 h, but needed to be much larger to 108 h to ensure 68% of the verifying WAIP intensity forecasts would be within the intensity spreads. However, the calibrated intensity spread at 156 h is only ± 10 kt (Fig. 1c) because all of these storms must by definition end prior to 168 h, and thus are more homogeneous in intensities so an intensity spread of only 10 kt still encompasses 68% of the

WAIP ending storm intensities. The calibration of the intensity spreads for this independent set is again quite successful as most of the PoDs are within 5% within the desired 68%. After this calibration, the mean intensity spreads are smaller from 12 to 54 h but have to be larger at longer forecast intervals to ensure the WAIP intensity spreads encompass the desired 68% of the verifying intensities (Fig. 1d). Thus some extra effort by the forecasters to identify ending storm events such as TC landfall within 7 days will allow improved intensity and intensity spread forecast guidance.

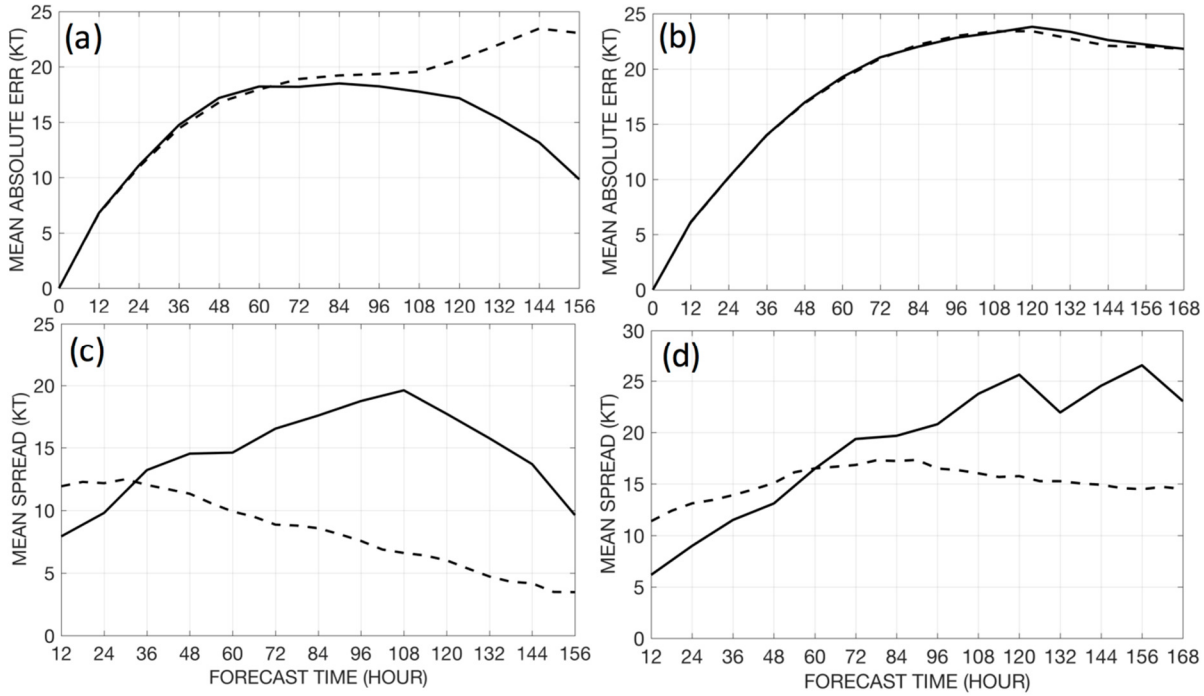

Figure 1*. Mean Absolute Errors (MAEs, kt) for independent sets of (a) Ending Storm subsample and (b) Non-ending storm subsample when the separate bias corrections are applied (solid line) or the All Sample (including both ending and non-ending storms) bias corrections are applied (dashed line). (c) and d) As in panels (a) and (b) except for the mean intensity spreads (kt) before (dashed line) or after (solid line) applying a calibration of the raw intensity spreads to these independent sets.*

For development and testing of the ending storm version of WAIP, the ending time is given by the JTWC best track file. In an operational application, the forecaster will need to provide this ending time. After the forecaster has made the 7-day TC track forecast, the forecaster will evaluate if the TC will end at any time along this 7-day track forecast due to landfall. With this new ending storm WAIP version on a desktop computer, within minutes the forecaster could easily vary the landfall time to take into account likely along-track forecast errors and thus see the impacts on the WAIP intensity and intensity spread forecast. Such techniques may ameliorate the challenges associated with longer-term forecasts produced by regional NWP models.

3. Recent advances in TC observing systems

On 15 December 2016, the U.S. National Aeronautical and Space Administration (NASA) deployed the Cyclone Global Navigation Satellite System (CYGNSS). The primary objectives of CYGNSS are to measure the ocean surface wind speed (but not direction) in the TC inner core (i) in all precipitating conditions (unlike scatterometers that are contaminated by heavy rain) and (ii) from formation through rapid intensification to decay and extratropical transition between 38°S and 38°N.

The CYGNSS mission is comprised of eight Low Earth Orbiting (LEO) spacecraft at an inclination of 35° which receive both direct and reflected signals from Global Positioning System (GPS) satellites. The direct signals pinpoint LEO spacecraft positions while the reflected signals respond to ocean surface roughness from which ocean surface wind speeds may be retrieved. Each spacecraft is capable of measuring four simultaneous reflections, producing 32 surface wind measurements per second from the constellation of eight. As the spacecraft are separated some distance in orbit, their 32 ground tracks over 90 minutes are spread in latitude and longitude along the orbital path (Fig. 2). As these GPS signals are at a long (L-band) wavelength unaffected by precipitation, surface wind speed estimates can theoretically be obtained in the TC eyewall region.

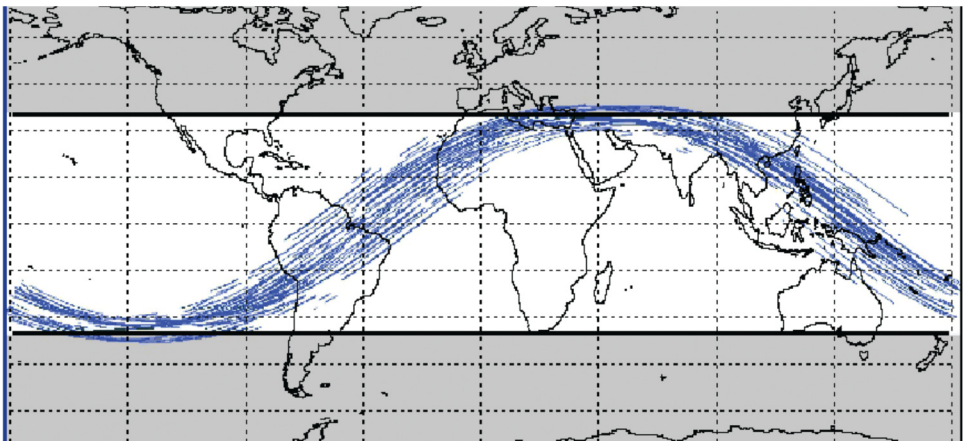

***Figure 2**. 90-minute coverage of the eight CYGNSS spacecraft. They are positioned in low earth orbit at an inclination of 35°.*

Given the varying positions of the eight spacecraft, it is possible for one of the eight to pass directly over the center of the TC but the neighboring spacecraft to miss the center. It thus becomes challenging to combine the surface wind speeds observed by other spacecraft to create a complete analysis of the TC wind field. However, at least one algorithm has been developed and tested with simulated data, and efforts are underway to use reconnaissance and research aircraft to collect observations during CYGNSS overflights. Even when coincident aircraft measurements are collected (say over several hours) within the region covered by the CYGNSS spacecraft that will pass over in 30 minutes, calibration will not be an easy task. Also, the greatest limitation of the CYGNSS mission is that only eight spacecraft are in orbit. While the swath coverage over 90 minutes (Fig. 2) may be adequate for a TC at 30°N, the longitudinal spacing between the eight spacecraft grows progressively larger toward the equator. The median revisit time is around 3 hours while the mean revisit time is around 7 hours.

Real-time collection of the CYGNSS surface wind measurements are not presently occurring due to logistical limitations. Only three ground stations download the 32 large datasets of one second observations. The CYGNSS was launched as a research satellite on a limited budget, and that budget currently limits downloads to once every day or two. Clearly, more ground stations or more frequent data downloads are required to do real-time collection, and NASA is exploring other options. However, once these logistical issues are resolved and the calibration phase is completed, two-dimensional analyses of CYGNSS surface wind speed, including the TC inner cores, will be made publically available. There are also several promising efforts to analyze vortex structure (e.g., wind radii of 34 kt, 50 kt, and 64 kt) and even TC intensity on occasion. At first, these vortex structures will only be available for post-storm validations. If the limitations of numbers of spacecraft, ground-station availability, and data download costs and capacity can be overcome, forecasters and researchers will have a new source of TC intensity and structure observations.

4. Track changes

Accurate forecasts of changes in TC track near land can depend on small-scale features such as topography. TCs are frequently deflected from their original direction of motion when they approach mountain ranges and other types of complex terrain. For example, both TC direction and size impact track deflections when these storms approach Taiwan. Northward-moving TCs slow down and are first deflected southwestward, then northward. When Chinese terrain is added to the simulations, the northward deflection is reduced, but the southwestward shift is enhanced (Tang and Chan 2014). With respect to TC size, the remote topographic effect for smaller TCs is weaker; that is, a TC must move closer to Taiwan to be deflected (Tang and Chan 2015). Finally, Tang and Chan (2016) examined the sensitivity to different steering flow strengths. In their previous studies, the TCs approached Taiwan just due to the beta-effect. In this study, different steering flows were added (5 m s^{-1} and 10 m s^{-1} easterly flow). Broadly, weaker steering flow was correlated with larger track deflections.

For typhoons making landfall in Taiwan, Wu et al. (2015) found northerly asymmetric flow in the middle troposphere was the leading factor in the southward deflection for an easterly moving TC approaching Taiwan, which is different from the low-level channeling effect. Sensitivity tests showed intense TCs experience greater southward deflections prior to landfall when the mountain is higher, when the vortex approaches the northern and middle portion of the terrain, or when the storm moves slower.

Topographical track deflections are not restricted to the western North Pacific. Barbary et al. (2017) showed track deflections may move a TC closer to La Réunion, possibly degrading weather conditions and increasing risks and potential damage. That study used RSMC La Réunion best tracks over the period 1981-2015 to quantify the distance of influence of the island on storm direction, speed, and intensity for all systems located within 100 to 1800 km radius of the island center. Statistical tests showed La Reunion's topography alters storm movement within 380 km of the island; that distance decreases to 250 km for weak storms. La Réunion also generally induces storm weakening within a 50-km radius, while storms moving away from the island while within 250 km also tend to weaken.

In addition to the benefits of low track forecast errors for adequate public advisories and warnings, forecasts of TC-related floods depend on accurate track forecasts. Within the SPICy project, Météo-France designed a method to generate ensemble scenarios around the RSMC La Réunion official track forecast (Quetelard et al. 2018). First, a 5-year sample of RSMC La Réunion forecasts (position and intensity) is used to identify 40 clusters of typical errors for lead times of 0, 12, 24, 30, 42, 60, and 72 h through an ascending hierarchical classification. Each of the 40 classes is given a probability according to the number of sample forecasts that compose it. The 40 climatology-built forecasts are associated to quantified maximum wind and position departures from the official RSMC forecast. The ECMWF Ensemble Prediction System (EPS) forecast realigned on the RSMC official forecast is then considered to account for the event predictability. The 51 members are assigned to the nearest climatological class using Euclidean distances. This reduces the original set of 40 classes to some 15 or 30 scenarios depending on the meteorological situation. The probability of each scenario is given by that of the original climatological class weighted according to the number of EPS members that falls into it.

For each individual scenario, wind and pressure fields are generated through mesoscale modeling (French non-hydrostatic research model, Meso-NH) using a bogusing method that filters out the misplaced TC circulation and inserts a synthetic three-dimensional Holland vortex into the model

analysis. The bogus is constructed to fit real-time estimates of storm size and intensity. This high-resolution ensemble of wind and pressure fields can finally be used for (1) generating probabilistic products such as the chance of exceeding different wind thresholds (Fig. 3) and (2) forcing a wave model and/or a storm surge model and produce probabilistic forecast of oceanic and coastal conditions.

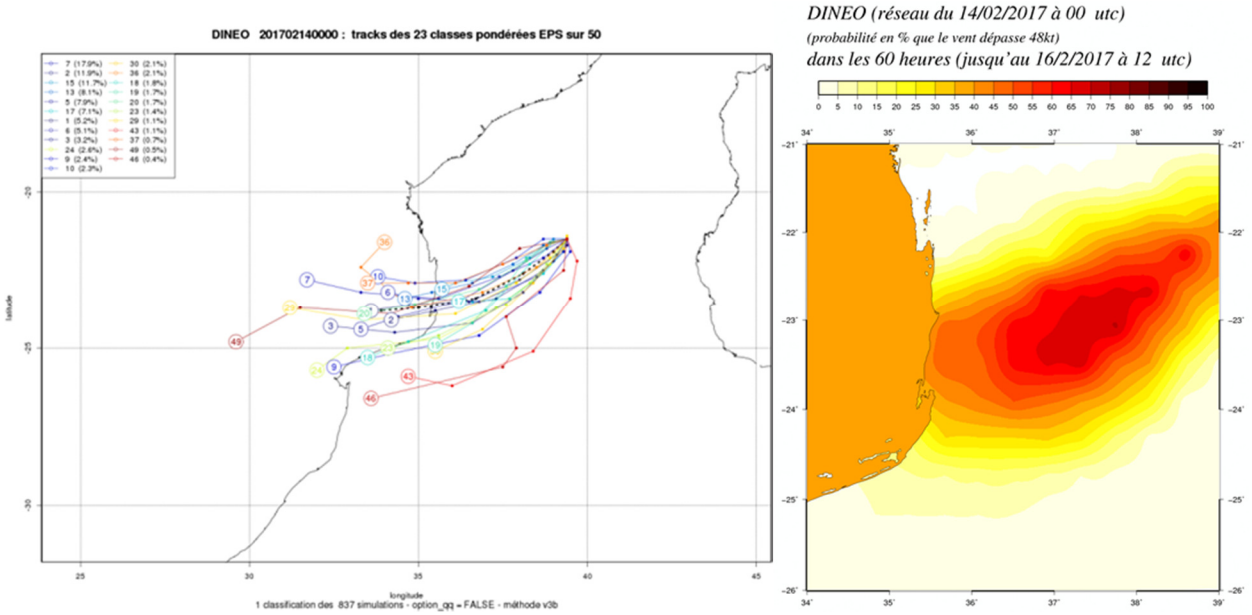

Figure 3*. (Left) Ensemble probabilistic track forecasts for TC Dineo (2017) making landfall in Mozambique. (Right) Chance (%) of winds exceeding a 48-kt threshold in the area for a 60-h period following 0000 UTC 14 Feb 2017.*

5. Numerical investigations of TCs near land

Recent numerical experiments have expanded our understanding of TC interactions with terrain as they approach land. Huang et al. (2016) used idealized simulations to investigate upstream track deflection of a propagating cyclonic vortex past an isolated mountain range, taking into account both boundary layer mixing and cloud effects. The direction of the upstream track deflection was determined by the ratio of the vortex size to the north-south length scale of the mountain range (for a westbound vortex). Deactivation or reduction in the boundary layer turbulent mixing and cloud effects reduce the southward deflection due to weaker channeling effects.

Lin et al. (2016) examined the orographic influence on track deflection via idealized simulations and vorticity budget analysis, where the vorticity budget analysis is used to predict TC motion using the vorticity tendency. For a westbound vortex, TC track deflection was explained by: 1) upstream deceleration due to orographic blocking, causing a southward advection of the TC, 2) anticyclonic motion of the TC as it passes the mountain, and 3) northwest movement on the lee slope which may be abrupt (Fig. 4).

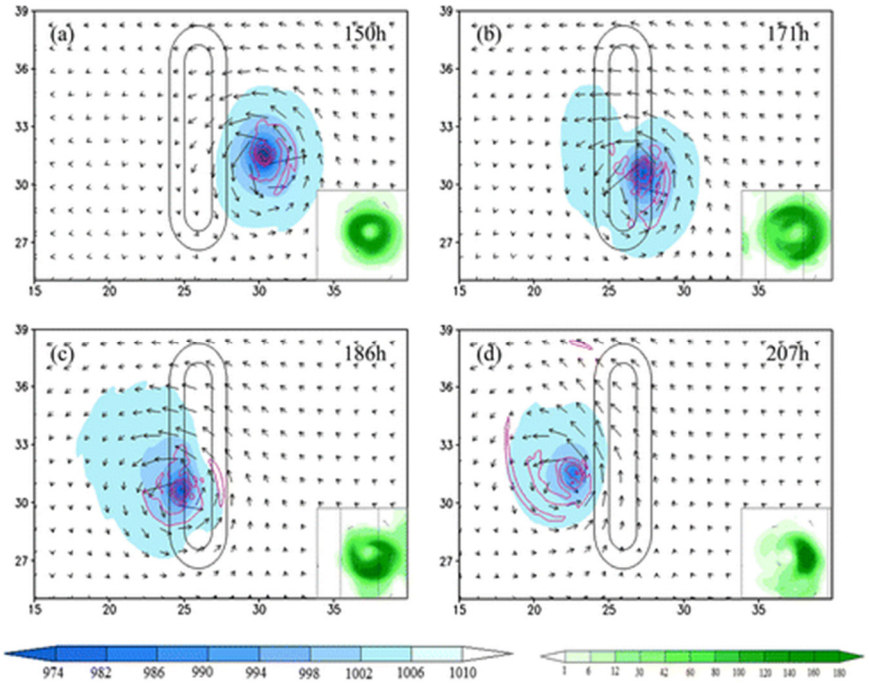

***Figure 4**. Track deflection of a westbound TC approaching a north-south oriented mountain range. The 3-h accumulated rainfall is in green, the surface pressure is shaded in blue, and the relative vorticity is contoured in red. Reproduced from Lin et al. (2016).*

In addition, Huang et al. (2016) found that conceptual models can be constructed from numerical experiments. For example, when a typhoon is passing a shorter mountain range, it may experience an early northward deflection prior to landfall and then take a sudden southward turn as it gets closer to the mountain range in response to the effects of the stronger northerly wind over the mountain due to the effects of channeling flow.

Due to the discovery of La Reunion's topographical influences on TCs (Barbary et al. 2017), a hierarchy of idealized simulations at 4-km resolution was performed with the French non-hydrostatic research model (Meso-NH). The island effect is shown to be more pronounced when the idealized TC is within 100 km of the island. In this scenario, storm speed increases when approaching the mountainous island. The track is deflected toward the terrain while the storm central pressure increases by some 7 hPa, starting at less than 100 km (that weakening is more pronounced and starts earlier in the case of more mountainous terrain compared to a flat island). The vortex temporarily slows down after passing over the island, which may cause a blocking effect in the leeward side of the terrain. Finally, the vortex accelerates while moving away from the island and re-intensifies. With imposed trade winds of 5 m s^{-1}, TC speed and direction changes occur within a 24-h period, and 6-hourly observations are theoretically sufficient to detect the terrain effect. Unfortunately, the track changes of systems passing the island at greater distances or embedded in faster flow may go undetected in the 6-hourly best-track database.

Due to the impacts of monsoon gyres on TC behavior and the potential for these interactions to occur near land, Liang and Wu (2015) used idealized WRF simulations to investigate the dynamics associated with these interactions. An approaching TC will cause the monsoon gyre to move northwestward, but the gyre's circulation will cyclonically rotate the TC's beta gyres, slowing the TC's initial northwestward movement. As the TC center becomes collocated with the monsoon gyre center, the energy dispersion associated with the symmetric TC circulation is enhanced, and the negative relative vorticity rapidly strengthens southerly winds in the eastern periphery of the TC. The resulting steering makes the TC take a sudden northward track.

Liang and Wu (2015) also found that TCs initially located in the eastern semicircle of monsoon gyres generally move in three directions: a sudden northward track, a westward track, and a northward track without a sharp turn (Fig. 5). The track types depend upon the TC movement relative to the gyre center. Westward TCs move faster than monsoon gyres and are then located to the west of the gyre center, while TCs that move more slowly than the gyres take a northward track without a sharp turn. This study reveals the specific TC track in the eastern semicircle of a monsoon gyre is sensitive to the initial wind profiles of both the gyre and the TC.

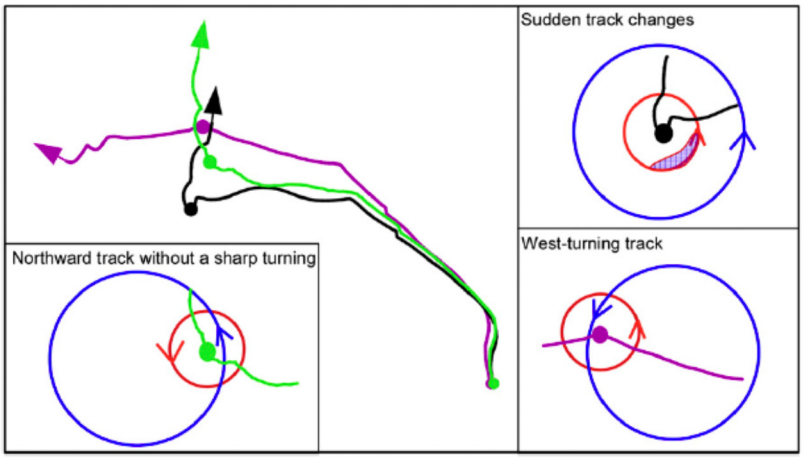

***Figure 5**. Schematic diagrams of three track types of TCs interacting with a monsoon gyre. The blue and red circles with arrows denote the gyre and TC circulation, respectively.*

6. Intensity changes

As mentioned in the Introduction, while intensity forecasts have improved in recent years (e.g., DeMaria et al. 2014), rapid intensity change remains a source of error. Coastal preparations strongly depend on accurate intensity forecasts, and rapid intensity changes near land can impact these preparations as well as public perception of forecast accuracy. In addition, the TC's current intensity impacts future rates of positive intensity change: Qin et al. (2016) demonstrated the intensification rate for hurricanes at the 90th-95th percentile decreases as TC intensity increases from category 3 to category 5. This supports Xu and Wang (2015), who also found the intensification rate of North Atlantic (NATL) TCs peaks at 70-80 kt (maximum 1-min sustained wind speed).

Recent climatological studies of intensity changes and near-land intensity changes in different tropical regions have quantified the possible range of TC intensification and decay in these locations. Leroux et al. (2017) established SWIO thresholds of rapid intensification (RI) and rapid decay (RD). Similar to the 30-kt threshold commonly used in the North Atlantic basin for 1-min sustained wind speeds, RI is statistically defined by a 24-h minimum increase of 15.4 m s^{-1} in the maximum 10-min sustained wind speed. RI is most common for TCs with initial intensities between 65 and 75 kt. RD is defined as a minimum weakening of 13.9 m s^{-1}, although this threshold may not be appropriate for all systems. Operational intensity forecast errors are significantly larger for RI events at short lead times (10.8 m s^{-1} versus 4.9 m s^{-1} for non-RI events at 24 h).

Using 133 TCs that made landfall in China from 2001 to 2015, Yu et al. (2017) found an average intensity decrease from 34 m s^{-1} before landfall to 20 m s^{-1} 24 h after landfall. Though the average minimum pressure remained steady 6-12 h prior to landfall, they noted the changes in pressure did not strictly follow the changes in maximum wind speed in some cases (Fig. 6). This suggests the wind-pressure relationship may not remain constant prior to each TC landfall. In addition, most TCs that hit

China have nearly steady if not increasing intensity prior to landfall and then exhibit the most rapid intensity decrease in the first 6 h after landfall.

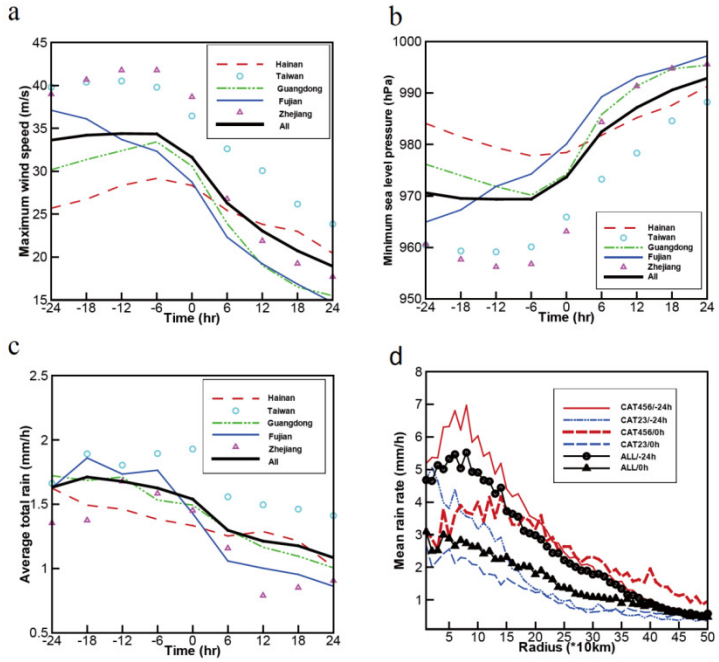

***Figure 6**. Six-hourly evolution for 133 TCs from 24 h prior to landfall to 24 h after landfall for (a) the average maximum sustained 10-m wind speed, (b) the average minimum sea level pressure, and (c) the areal average rain rate within a 500-km radius of the storm center. (d) Radial profiles of the azimuthally averaged rain rates for different TC intensity groups.*

Though rapid intensification remains a major contributor to intensity forecast errors, rapid weakening also tends to increase these errors. Using National Hurricane Center data for the NATL and eastern North Pacific (ENP), Wood and Ritchie (2015) showed greater error for 24-h rapid weakening events compared to slower weakening periods. These events were associated with negative sea surface temperature gradients, increasing vertical wind shear, and dry air intrusions. While their study focused on weakening when the TC center was at least 50 km from land, these rapid intensity changes can occur near land and thus affect both coastal preparation as well as public perception of forecast accuracy.

The intensity of TCs interacting with large-scale monsoon gyres is often affected by changes in TC structure. Liang et al. (2016, 2017a) applied an observational analysis to WNP TCs and noted the important effect of monsoon gyres on rapid weakening. The rapid weakening of Typhoon Chan-Hom (2015) occurred when it coalesced with a low-frequency (15-30 days) monsoon gyre. The interaction between these two systems induced the development of strong convection on the eastern side of the monsoon gyre, which prevented inward transport of mass and moisture into the TC, leading to the collapse of the eastern part of the eyewall. Liang et al. (2017b) performed a composite observational study to examine rapid weakening events occurring in monsoon gyres in the tropical WNP basin during May-October 2000-2014. More than 40% of rapid weakening events south of 25°N were observed near the center of monsoon gyres and accompanied by a sudden northward turn, yet the large-scale environmental factors did not have primary contributions to that weakening.

Size can impact a TC's potential for intensity change, yet the Dvorak technique is often limited for small TCs. Satellite observations indicate the size of a system is only weakly correlated to its intensity (Chavas and Emanuel 2010). Recent examples of small but intense SWIO TCs include Fantala (2016) and Hellen (2014), two of the most intense systems ever recorded in the basin. Over the 2010-2016 period, the 5th percentile of 34-kt wind radii (R34) for SWIO TCs was 46 km, which was defined as the radius for a midget TC (Leroux et al. 2017). On average, these midget systems are weaker and have smaller inner

cores, consistent with their small R34 values. However, they are more likely to undergo RI and RD, possibly due to greater sensitivity to their environments. A larger midget system sample is needed to assess operational forecast errors regarding the challenge these midget systems represent for intensity and track prediction.

Environmental factors also affect TC intensity, such as eddy flux convergence (EFC) of angular momentum and vertical wind shear. However, their effects appear to be unequal. Using ECMWF reanalysis data, Peirano et al. (2016) analyzed NATL TCs from 1979 to 2014 and found trough-induced EFC was a weak predictor of intensity change compared to trough-induced vertical wind shear (Fig. 7). This may be important for improving intensity forecasts of TCs near troughs, particularly if those TCs are also approaching land.

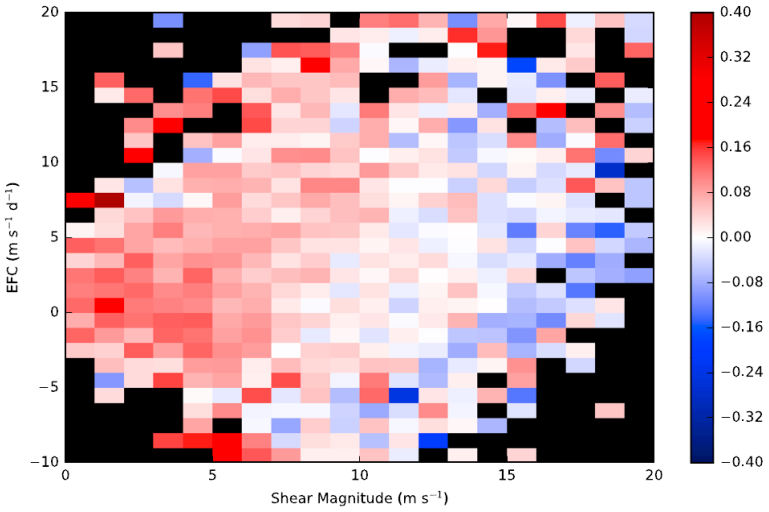

***Figure 7**. Mean 24-h dimensionless intensity change (shaded) for all eligible TC periods binned by 850–200 hPa vertical wind shear and 300–600 km eddy flux convergence at 200 hPa. Black indicates no data. Adapted from Peirano et al. (2016).*

7. Impacts of TC structure and structural changes near land

Kosiba and Wurman (2014) extended Kosiba et al. (2013) by examining the boundary-layer structure of Hurricane Frances (2004) at landfall using the Doppler on Wheels (DOW) mobile radar, observing linear coherent structures with a characteristic wavelength of 400-500 m (Fig. 8). They found the vertical flux of horizontal momentum caused by individual vortical structures was substantially higher than values employed in turbulence parameterization schemes. However, when considering the domain-wide average flux, it was substantially lower than that in individual structures, likely due to the transient nature of the most intense portions of the structures.

Zhang et al. (2017) used numerical simulations to examine the effects of boundary layer vertical mixing on hurricane simulations over land. For real case simulations, it was found that stronger vertical mixing in the boundary layer at landfall led to improved prediction of track, intensity, and structure. Weaker vertical mixing produced hurricanes that were too strong over land.

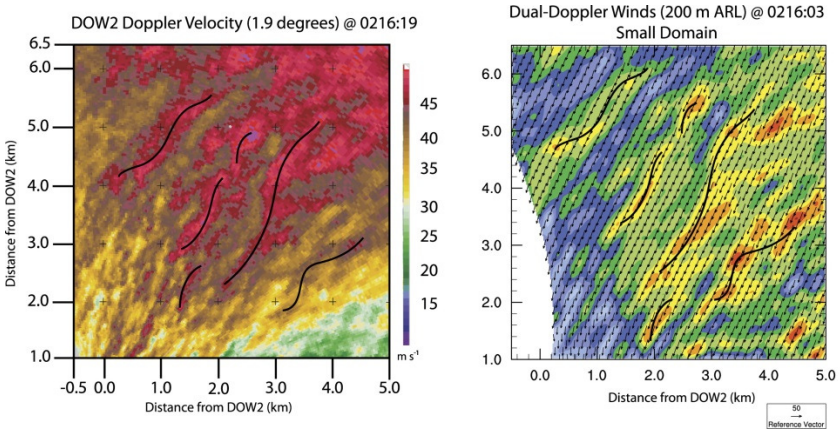

***Figure 8**. Dual Doppler raw velocity data (left) and syntheses on a domain (right). Wind streaks are noted by black lines. Reproduced from Kosiba and Wurman (2014).*

Stronger and larger TCs have larger average spatial coverage of rainfall and higher average rain rates (Yu et al. 2017). However, extreme rainfall can occur at large distances from the center when a landfalling TC interacts with its environment. Many observational and modeling studies have highlighted the critical physical processes in changing TC structure and precipitation at landfall. These include variability in low-level moisture transport, changes in boundary layer frictional convergence, low-level frontogenesis, upper-level outflow layer divergence, and atmospheric instability (Wang et al. 2009, Moore et al. 2013; Milrad et al., 2013; Riemer and Laliberté 2015).

These TC-environment interactions are not necessarily restricted to the outflow layer and the boundary layer, as they can also occur in the mid-levels of the TC circulation. Bao et al. (2015) used trajectories to analyze landfalling Typhoon Fitow (2013), which produced more than 300 mm of rainfall in a day 400 km north of the center. A large percentage of the air within the high rain regions was traced back to the environment, and high PV air entered the region through the mid-levels when Fitow interacted with a trough. Deng et al. (2017) investigated Tropical Storm Bilis (2006), which produced torrential rain 400 km southwest of the center after landfall in China, rainfall not included in the forecast. They found the increased deformation and weakening of vertical vorticity as Bilis approached the monsoon trough contributed to the storm evolving from a closed, tight circulation into a loosely-distributed circulation. As a result of the induced pressure and wind anomalies induced by this structure change, an increase in gradient wind imbalance in the mid-levels re-distributed high PV air from the inner core to outer radii. This redistribution of PV explained the rapid decline of the inner core circulation and provided a direct lifting mechanism for convection within the outer rainband over land.

Within numerical simulations, horizontal resolution can impact model depictions of intensity and structure in intense typhoons. When investigating Typhoon Rammasun (2014), Wang and Zeng (2017) produced a stronger simulated TC as the resolution increased, yet even the finest resolution (3 km) still underestimated Rammasun's peak intensity. Also, as horizontal resolution increased, Rammasun's vortex contracted horizontally and deepened vertically with a thinner yet more intense eyewall and a stronger warm core. Increasing resolution from 9 km to 3 km produced much greater structural and intensity changes compared to the change from 15 km to 9 km, implying this resolution is crucial to properly resolving inner core features. Parameterization scheme changes had far less impact than resolution changes.

8. Operational practices and challenges

8.1 Philippine Atmospheric, Geophysical and Astronomical Services Administration (PAGASA)

Tropical Storm Tokage (2016), known as Marce in the Philippines, demonstrated challenges associated with a TC's abrupt change in direction on 26 November (Fig. 9). Average PAGASA forecast errors were 211, 276, and 546 km at 24, 48, and 72 hours, and the bulk of these errors can be attributed to Tokage's unexpected northeastward heading. Other meteorological centers predicted a shift in the track heading of Tokage (from westward to northward or northwestward) but not recurvature as they also expected the system to be embedded in the impending cold surge, forcing the TC to move generally southwestward once it weakened.

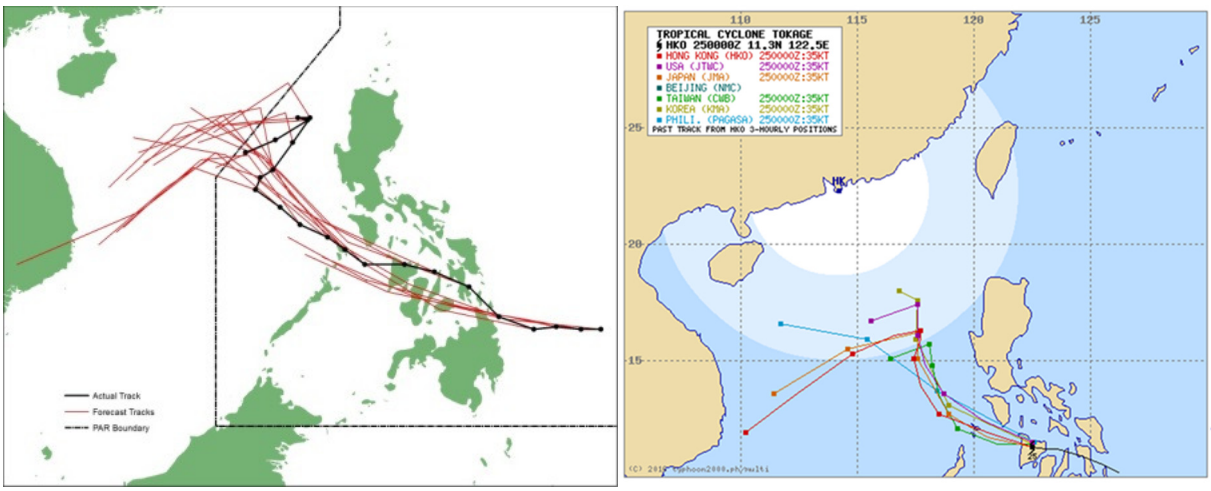

Figure 9*. (a) 3-day forecast tracks issued by PAGASA through the lifespan of Tropical Storm Tokage. (b) Forecast tracks of various TC warning centers at 00 UTC 25 November.*

Rapid intensity changes also reduce forecast accuracy. In 2016, Super Typhoon Haima (Lawin) encountered favorable atmospheric and oceanic conditions and rapidly intensified. However, PAGASA had predicted no significant intensity changes prior to landfall on Luzon's eastern coast. In response, PAGASA issued Tropical Cyclone Warning Signal 5, the highest value on the warning scale. But after Haima reached its peak intensity yet hours prior to its landfall, satellite observations revealed an eyewall replacement cycle was about to begin. In addition, strong vertical wind shear over Luzon was in Haima's direct path. By 1200 UTC, Haima weakened below Super Typhoon strength, and rapid weakening followed as its inner core interacted with mountainous terrain as the eyewall replacement cycle was near completion.

8.2 Joint Typhoon Warning Center (JTWC)

JTWC generates and distributes Significant Tropical Weather Advisories, Tropical Cyclone Formation Alerts, and TC track, intensity, and wind field forecasts for U.S. Government customers in the North Pacific, South Pacific, and Indian Ocean basins. Significant Tropical Weather Advisories classify the potential for tropical cyclone formation (TC) from monitored disturbances within a 24 hour forecast period as "low," "medium," or "high." Tropical Cyclone Formation Alerts provide a geographical area for potential TC formation of each disturbance at the "high" classification level. TC warnings cover a 120-h forecast period unless either dissipation or extratropical transition (ET) is expected to occur earlier. If either dissipation or ET is predicted, the JTWC warning will cover the period up to and including the anticipated dissipation or ET. Forecasts are issued every six hours. The 1-minute maximum sustained wind speed for initiating TC warnings is 25 knots in the North Pacific and 35 knots in the North Indian

Ocean and Southern Hemisphere, with allowance to “warn early” for timely protection of resources and human life.

The tools and methods that JTWC applies to analyze and forecast TC track, intensity and structure have continually improved over the past several years, reinforced by the transition of several new techniques from applied research into operations. Although satellite observation capabilities have also improved in some respects, there is uncertainty surrounding the future number and capabilities of TC-observing, low-earth orbiting satellites and component sensors.

JTWC forecasters continue to rely upon intensity estimates from the subjective Dvorak technique as well as data from both active and passive satellite sensors and multiple automated, objective intensity estimation techniques. Reliable active scatterometer data provided in near real-time from the ASCAT sensor onboard METOP-A and METOP-B satellites, and more recently from SCATSAT-1, facilitate the intensity analysis process for TCs in the tropical depression and tropical storm stages. Data from these platforms cover large geographic areas that are typically void of reliable in situ data.

In addition to subjective Dvorak estimates and scatterometer data, forecasters consider intensity estimates derived from multiple objective methods. These methods include recently-introduced intensity estimates that use data from the SSMIS (Hawkins et al. 2016) and ATMS (Herndon and Velden 2016) sensors, the Automated Dvorak Technique (ADT; Olander and Velden 2007) and the automated Satellite Intensity Consensus (SATCON; Velden et al 2006) provided by the University of Wisconsin Cooperative Institute for Meteorological Satellite Studies. These automated data are regularly referenced and applied during the intensity analysis process and have been particularly beneficial for identifying and confirming cases of rapid intensity change (Fig. 10). These rapid intensity changes may be otherwise underestimated, in some cases, due to “constraints” inherent to the subjective Dvorak analysis technique and other factors.

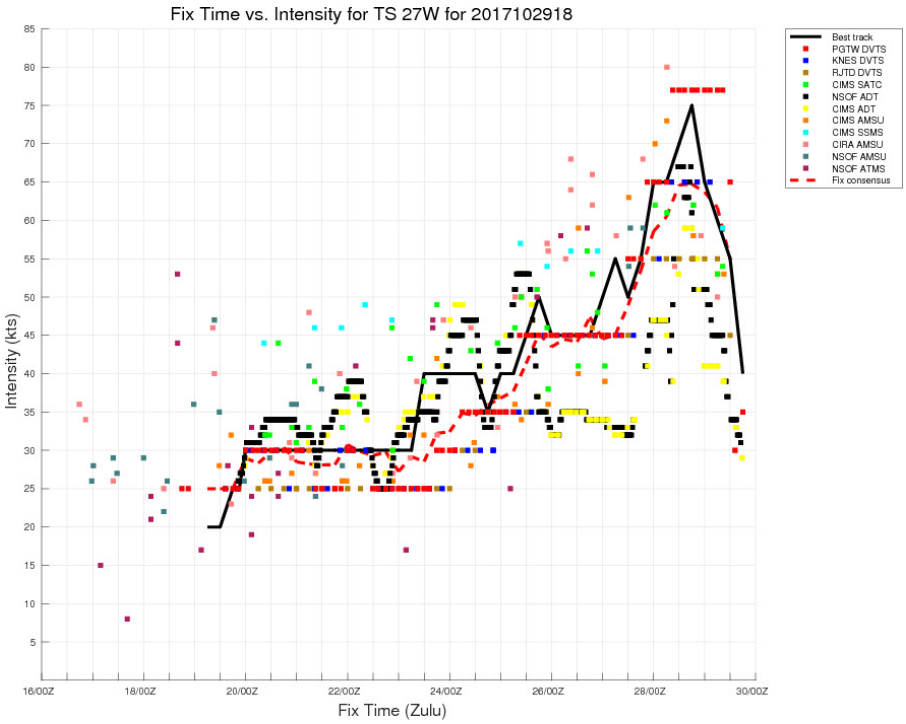

***Figure 10**. Example intensity time history for TC 27W (2017) showing the intensity analysis estimates currently available to the JTWC forecaster. All estimates listed in the label from “CIMS SATC” (CIMSS SATCON) down are based on automated analysis techniques. These estimates facilitate intensity analysis in open-ocean and near-landfall scenarios alike. Further refinements to these techniques will increase intensity analysis accuracy.*

JTWC applies a suite and consensus of intensity forecasts derived from statistical-dynamical techniques and dynamical models as the primary objective aid for forecasting TC intensity. Several new tools and techniques designed to both improve intensity prediction in general and to quantity the potential for rapid intensification have been introduced at JTWC. These include probabilistic intensity forecast spreads predicted by the Goerss Predicted Consensus Error (Goerss and Sampson 2014) and Weighted Analog Intensity methods (Tsai and Elsberry 2015). By providing upper and lower "bounds" to intensity forecasts, these methods lend forecasters insight regarding the potential for rapid intensity change that may not be readily discerned from individual model forecasts or the consensus alone. Intensity forecasts from mesoscale model ensembles, such as the COAMPS-TC (Doyle et al. 2012) ensemble, could further augment and refine available intensity spread guidance. JTWC has also implemented updated probabilistic rapid intensification guidance from the Statistical Hurricane Intensity Prediction Scheme (SHIPS-RII) (Kaplan et al. 2010) and passive microwave imagery analyses (Kieper and Jiang 2012).

JTWC has implemented several new techniques to analyze and forecast TC structure over the past few years. For example, forecasters now consider an "analysis consensus" composed of satellite-derived automated wind field estimates, dynamic model analysis wind fields, and wind radii derived from the agency's most recent Dvorak intensity fix data when formulating 34-kt, 50-kt, and 64-kt wind radii analyses (Knaff et al. 2016) (Fig. 11). Additionally, a multi-model consensus of dynamical and statistical-dynamical model surface wind forecasts has replaced a climatology and persistence model as the primary tool for wind radii forecasting (Sampson and Knaff 2015) (Fig. 11). Statistical analyses indicate that both analyses and forecasts of gale-force (34-kt) wind radii issued by JTWC have improved following the introduction of these new tools. However, analyzing and forecasting 50-kt and 64-kt wind radii is more complicated given challenges associated with observing and predicting TC core structure. A statistical-dynamical approach to forecasting 50-kt and 64-kt wind radii has shown promise and will be tested at JTWC in the near future. Additional tools to accurately analyze and predict destructive wind radii near the core of TCs, where destructive potential is most potent, are still needed.

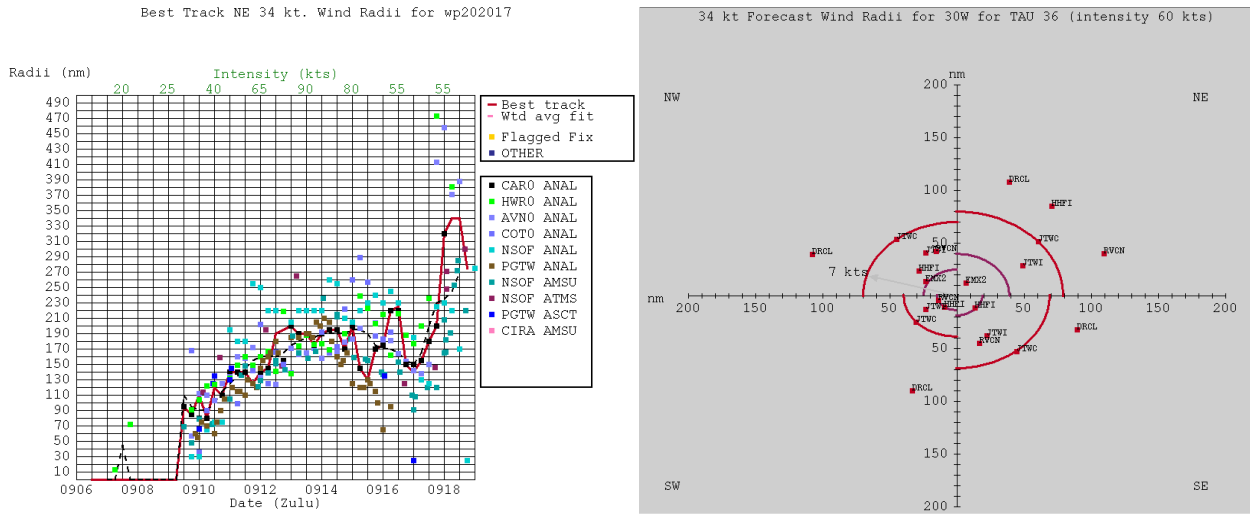

Figure 11. *(Left) Example wind radii analysis time history (TC 20W, 2017) showing the various estimates and objective consensus values available to the forecaster. (Right) Example wind radii forecast plot (TC 30W, 2017) showing forecaster-selected 34-kt (outer) and 50-kt (inner) wind radii by quadrant along with wind radii forecast consensus component model and other estimates.*

8.3 Taiwan's Central Weather Bureau (CWB)

The Taiwan Central Weather Bureau (CWB) has recently improved their Typhoon Weather Research and Forecast (TWRF) model (Chen et al. 2017), which uses Global Forecast System (GFS) input data (Fig. 12). These modifications were made in cooperation with the WRF development group at the National Center for Atmospheric Research. Rather than incorporating a bogus vortex, the application of "partial cycling" (Hsiao et al. 2012) improved TC initialization in TWRF. The model is initialized using a "cold start" from t-12 h with a simple interpolation of the GFS fields to the TWRF grid. After a 6-h forward integration of the TWRF model, a "blending scheme" generates a new initial field. The blended scheme is weighted toward the NCEP GFS for scales greater than the cutoff length of 1200 km and toward the TWRF regional field for smaller scales. The large-scale fields from GFS surpass the TWRF analysis, which significantly improves the typhoon track forecasts. On the other hand, the regional TWRF analysis provides a well-developed typhoon structure and more accurately captures the influence of the Taiwan topography on the TC circulation (Hsiao et al. 2015). The TWRF is then integrated to t = 0 h, and the blending scheme with the filtered GFS analysis at t = 0 h completes the initialization step. This approach allows a smooth start to the real forecast because the inner-domain fields are dynamically and thermodynamically balanced, and no TC bogus vortex is applied. Earlier uses of TC bogusing in TWRF resulted in unbalanced fields and larger track forecast errors compared to the partial cycling method.

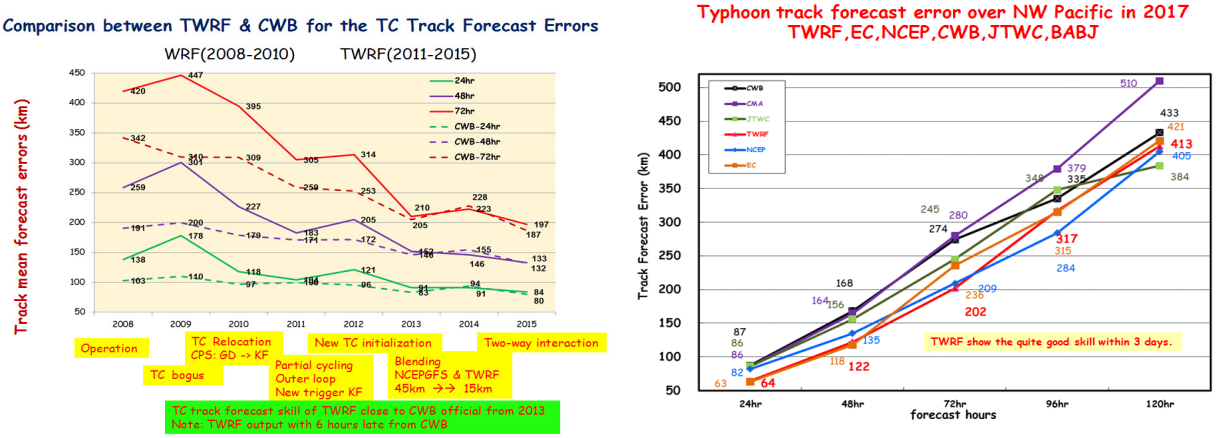

Figure 12. *(Left) Inhomogeneous comparison between TWRF and CWB official TC track forecast errors. Yellow and green highlighted text show the modifications from 2008-2010 (original WRF) to 2011-2015 (TWRF). (Right) Comparisons between TWRF, ECMWF, NCEP (GFS), CWB, JTWC, and CMA official track forecast errors in 2017 (through November).*

An additional TWRF improvement came from the installation of a new Fujitsu computer that has 92 times the capability of the previous computer. This allowed the new version of TWRF to have two domains with finer resolution: a 15-km outer grid of 662 x 386 grid points and a 3-km inner grid of 1161 x 676 grid points. Beyond improved representation of the TC inner core, the 3-km grid better resolves the topography of the Taiwan Central Mountain Range (CMR) and land-sea boundaries. The 3-km TWRF domain also encompasses the formation and decay areas of most TCs that might impact Taiwan, the Philippines, and Hong Kong. This expanded coverage may have motivated PAGASA to request additional CWB guidance products and for the Hong Kong Observatory to explore installing TWRF on their computer.

Compared to the previous version of TWRF, the 3-km grid has improved track forecasts as well. During the 2016 typhoon season, TWRF track forecasts were essentially as accurate as ECMWF forecasts. Through November 2017, many TWRF forecasts were more accurate than ECMWF (Fig. 12a).

Reduced error extends to intensity forecasts, which is likely due in part to increased spatial resolution. However, TWRF tends to overpredict intensity, particularly for slow-moving TCs (e.g., Lionrock in 2016), which may be due to the lack of TC-ocean coupling (Fig. 13). CWB is currently testing a one-dimensional upper-ocean mixed-layer model to improve this bias.

A key objective for the new 3-km grid over the CMR is to improve TC-related rainfall prediction due to the potential for heavy rain rates and large spatial variability. In addition to predicting potential flooding, water resource management in Taiwan depends on TC rainfall, and TWRF shows promise in meeting this objective (Fig. 14). Ensemble approaches have also demonstrated merit as shown by Hong et al. (2015). Ensemble typhoon quantitative precipitation forecasts (ETQPF) are obtained by averaging carefully selected cases from an ensemble prediction system with 38 members. Qualitative comparisons and quantitative verifications show ETQPF output provide reasonable typhoon rainfall forecasts and thus have value in real-time operational applications (Fig. 14). An online COMET/NOAA module based on the competency of using ETQPF (available in traditional Chinese) introduces the typhoon QPF methodology used by CWB (https://www.meted.ucar.edu/tropical/typhoon_qpf/).

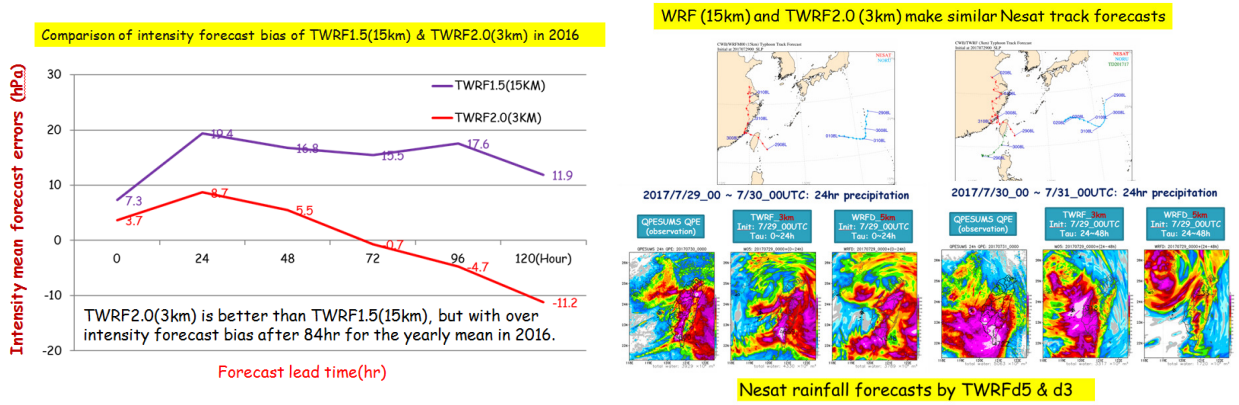

Figure 13. *(Left) Intensity forecast bias of TWRF1.5 (15km) and TWRF2.0 (3km) in 2016. (Right) Track and rainfall forecasts for Typhoon Nesat. TWRF2.0 showed more reasonable rainfall structure and distribution than TWRF1.5.*

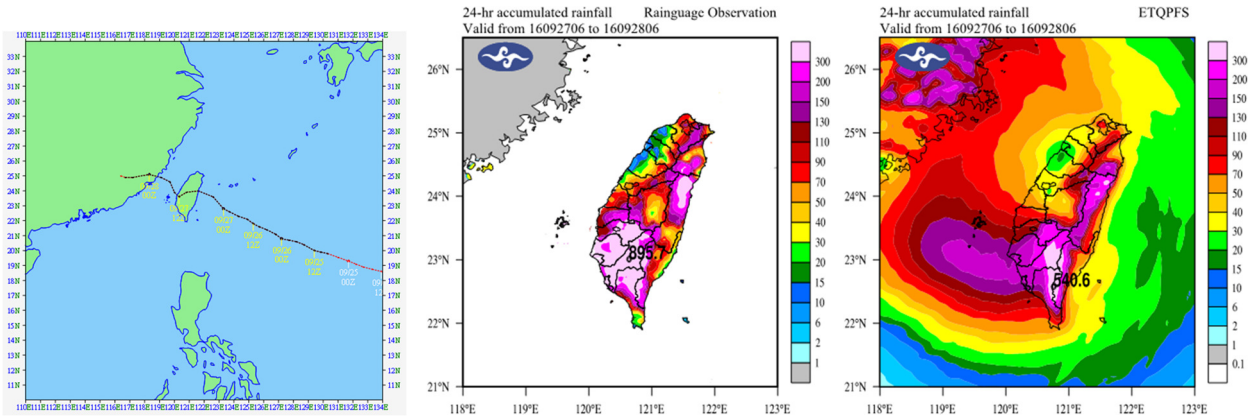

Figure 14. *(Left) Best track for Typhoon Megi (2016). (Center) 24-h accumulated observed rainfall (mm; starting 0600 UTC 27 Sep 2016). (Right) 24-h accumulated ETQPF rainfall (mm; starting 0600 UTC 27 Sep 2016).*

8.4 Australian Bureau of Meteorology (BoM)

Cyclone Marcia (2015) was a strong TC that directly impacted the coast of Queensland. Models showed good agreement regarding the track change near Creal Reef (Fig. 15). However, the TC's growing intensity as it appeared to approach populated and vulnerable locations such as Mackay prompted increased threat messaging for that area. Note that, in the final track, Mackay ended up outside the region of gale-force winds (Fig. 15).

Marcia provides an example of a great forecast, but not all events are predicted this well. How can forecasters efficiently make accurate determinations with the amount of information currently available? What procedures should they follow to ensure their forecasts use all the information in the most reliable ways within the time constraints of making a forecast? And what role should ensemble forecasts play in those procedures?

Another key question raised by Marcia is what buffers do emergency managers build around BoM forecasts when they see this sort of track change within a TC forecast? Should they blindly follow the BoM forecast or create contingency plans reflecting the level of uncertainty in the forecast?

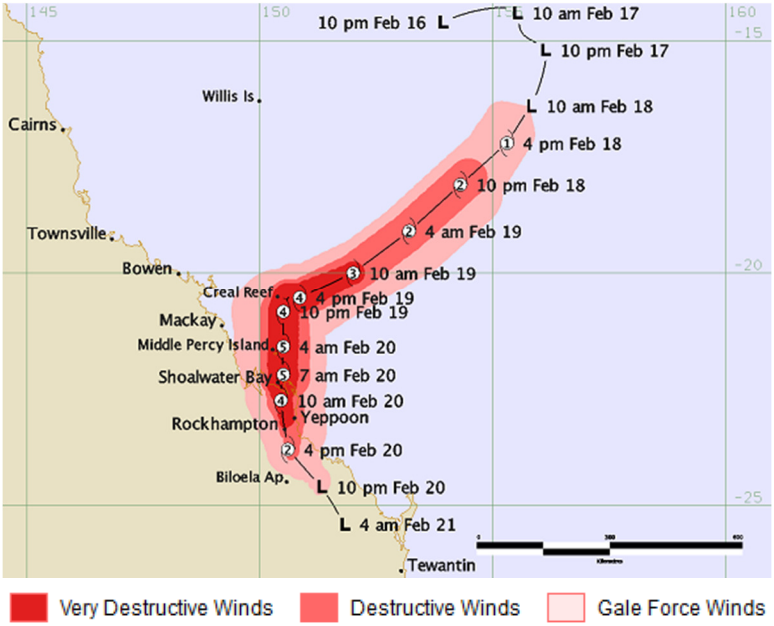

Figure 15*. Track of Cyclone Marcia (2015) and its associated winds.*

8.5 RSMC La Réunion

TC Hellen (2014) challenged TC intensity prediction as it threatened the Comoros archipelago and the Malagasy northwest coastline and became one of the strongest tropical cyclones ever observed in the SWIO. According to RSMC best track data based on Dvorak estimates (Dvorak 1984), the system gained nearly 70 kt (36 m s^{-1}) in 24 h, reaching a peak intensity of 125 kt (64 m s^{-1}) 132 km away from the coast. It then weakened at an even greater rate, 90 kt (46 m s^{-1}) in the following 24 hours while remaining over open water and thus made landfall as a weak tropical storm (35 kt). In less than three days, Hellen went up and down the Dvorak scale, as TC forecasters chose to break the Dvorak constraints regarding intensity changes (no more than ± 2.0 current intensity points in 24 hours) to keep up with the major changes observed in the TC structure. These rapid intensity variations were likely allowed by the TC's small size (Colomb et al. 2017). Hellen exhibited a radius of outermost closed isobar

around 220 km, about half the climatological mean value computed in the SWIO (following the classification and characteristics of midget systems given by Leroux et al. 2017).

The steep TC intensity variations that occurred right before landfall were not well anticipated by operational forecasting models or by RSMC La Réunion forecasters. Although RI was supported by a generally conducive upper-level environment as well as high ocean heat content in the Mozambique Channel, the record-setting rapid weakening was not supported by usual large-scale predictors. However, the new non-hydrostatic fine-scale model built for the operational needs of RSMC La Réunion (AROME-IO, Bousquet et al. 2018) was able to closely reproduce Hellen's intensity variations during experimental tests. Using both the simulation and the few sounding observations, mid-level wind shear associated with dry air was the main cause of Hellen's collapse. In the lower levels, low θ_e air was flushed into the boundary layer ahead of the mid-tropospheric dry air. These θ_e injections depressed the near-core θ_e values, weakening the updrafts within the eyewall at both low and mid levels. The upper half of the warm core was ventilated more quickly than its lower half. The system rapidly weakened as the higher warm core had a greater influence on the surface pressure. These results illustrate the recent paradigms for intensity modification under the thermodynamic impact of vertical wind shear (Riemer et al. 2010; Onderlinde and Nolan 2017).

Although TC track and intensity forecasts have steadily improved, a great amount of uncertainty remains. RSMC La Réunion 3-day track forecasts convey uncertainty using circles of 75% probability around the RSMC official track forecast; circles are built using the dispersion of cyclone positions in the ECMWF Ensemble Prediction System (EPS) and translated at the RSMC official forecast position. This method takes into account the meteorological synoptic context and proved to be more skillful than using the climatological distribution of position error (Dupont et al. 2011). However, risk managers or public agencies need both a reliable forecast of the TC evolution and an estimation of the forecast uncertainty (e.g., probability of a given variable to reach an expected value) regarding the potential coastal impacts (e.g., devastating winds, torrential rain, marine and river inundations) which are tightly related to the storm track as well as the storm's structural and intensity evolution.

Additional guidance is provided to SWIO forecasters with the first empirical MPI-SST relationship for the SWIO basin, derived in the 22-29°C range, using BT data and daily optimally interpolated SST (OISST) data at 0.25° latitude-longitude resolution (Leroux et al. 2017). The derived empirical MPI implicitly includes the effect of the outflow temperature on storm intensity. The exponential function of the form $MPI = A / (1+e^{-B(SST-T0)})$ differs from that obtained in the NATL and WNP (Zeng et al. 2007; Gao et al. 2016) and from the (nearly) linear relationship found in the ENP and the Bay of Bengal. The 29°C cutoff reflects a specificity of the SWIO basin: the Mozambique Channel spawns systems over very warm waters (compared to the open ocean) but offers them very little room for intensification before landfall. To offer further guidance to the practical intensity forecasts over the SWIO and better anticipate intensity changes, a future study will use sophisticated statistical techniques (e.g., neural network, decision trees, multilinear regression of the most relevant environmental predictors) to deliver a statistical-dynamical tool for the prediction of TC intensity and/or the probability of RI at short range, similar to those developed in other basins (e.g., DeMaria and Kaplan 1994; Knaff et al. 2005; Kaplan et al. 2010; Gao and Chiu 2012).

Finally, track deflections imposed by nearby terrain add to forecast complexity. In 2017, Cyclone Enawo jogged to the northwest shortly before landfall, a track change not forecast by RSMC La Réunion. To complicate matters, this shift brought the TC outside the 75% cone of uncertainty for that forecast (Fig. 16). The intense cyclone caused at least 81 deaths and USD $20 million in damage.

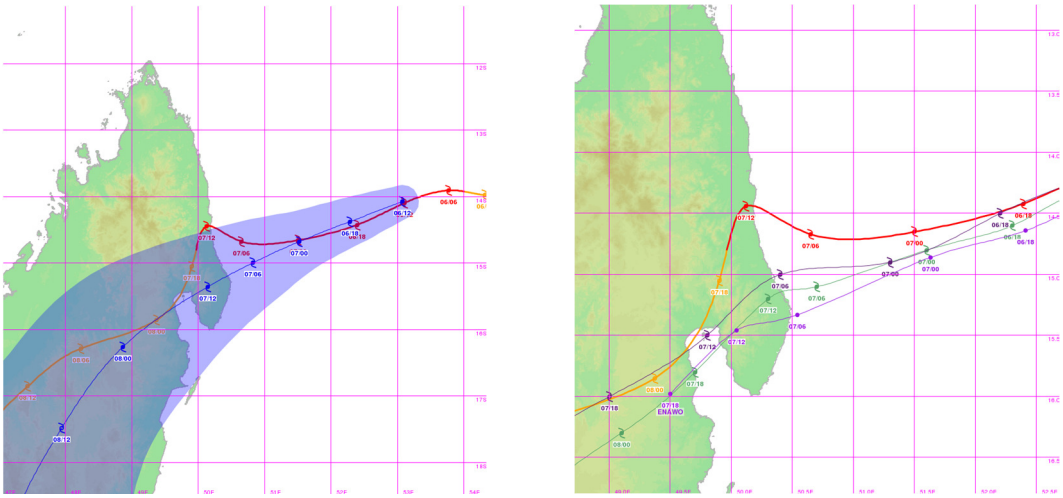

Figure 16*. (Left) Best track (red) and RSMC La Réunion official track forecast (blue) at 1200 UTC 06 March 2017 with EPS-based uncertainty circles of 75% probability (shaded area) for TC Enawo. (Right) Track forecasts from 0000 UTC 06 March 2017 for three numerical models: Arome-IO at 2.5-km resolution (light purple; southernmost track), GFDN (green), and HWRF (deep purple).*

9. Summary and potential for future research

This report presented a number of advances in understanding and prediction of TCs, particularly near land. Analog approaches show promise, particularly at long lead times (>5 days) and for systems near complex topography such as Taiwan. Higher resolution imagers on geostationary satellites (Himawari-8, GOES-16) are already assisting forecasters, and a new constellation of low earth orbit satellites may provide useful information on TC size and structure (CYGNSS). Track deflections due to topography and features such as monsoon gyres have been further investigated, and increased awareness of the dynamics behind these events may improve future forecasts. Improved understanding of track should reduce error in rainfall forecasts as well. Intensity change remains a challenge, with multiple recent examples of short-term intensity change near land causing difficulty, but continued improvements in both understanding and operational application should contribute to future forecast accuracy.

In situ observations are limited in the Indian Ocean, and organized field campaigns could provide insights and refinements to the methods used in the SWIO. In that regard, considerable efforts are currently being made to strengthen the means of TC observation in this particular basin through deploying new atmospheric and oceanic sensors. Experimental data will also be collected in the frame of the SWIO-TC experiment to be organized in the Mozambique Channel and Mascarene Archipelago in 2019. This field campaign, made in the frame of the EU-funded ReNov'Risk-Cyclones project, will provide unprecedented datasets in the SWIO basin by coordinating dedicated atmospheric and oceanic measurements, providing a unique framework to

i) better understand the physics of TCs over the SWIO and the relations between TCs and the large-scale atmospheric and oceanic environment;
ii) specifically calibrate for the SWIO the multiple satellite techniques, like the Dvorak technique, dedicated to TC detection and forecasting;
iii) objectively estimate TC forecast improvements due to the assimilation of additional data from surface stations, airborne measurements and satellite observations; and

iv) test the capabilities of high-resolution models to reliably reproduce the evolution of TC wind and precipitation structures as well as to predict their impact on the coastal regions of the SWIO.

Unfortunately, an anticipated decrease in the number of low-earth orbiting satellites carrying high-resolution imagers suited for observing TCs, particularly at microwave frequencies, will hinder JTWC's and other forecast agencies' capability to accurately analyze TC positions and detect rapid track changes. The development and deployment of satellites that carry these sensors and systems and provide their data through accessible outlets in near real-time is a high priority. Ongoing experiments with constellations of small satellites, including TROPICS and CYGNSS, offer a potential framework for providing economical microwave sensor coverage of TCs in the years ahead. Given forecasters' experiences with microwave-derived and/or automated satellite intensity estimates such as the ADT, continued progress in the development and refinement of automated TC intensity analysis is essential. In addition, we need to take advantage of improving observations from geostationary satellites due to their temporal coverage of large regions at risk of TC landfall. Of course, higher density in situ observations are also highly desired for both real-time analysis and verification.

Although quantitative guidance for predicting TC rapid intensification events is improving, more specific forecasts regarding the timing and extent of intensification are required, particularly for landfalling systems. Techniques to identify and isolate high probability extreme events – for example, 50 knots of intensification or greater within a 24-hour period – could mitigate losses in potentially catastrophic pre-landfall rapid intensification events (Fig. 17). In addition, rapid intensity changes are not limited to the 24-h time frame. Other time frames should be considered in all basins, but shorter time frames require observations at greater temporal resolution.

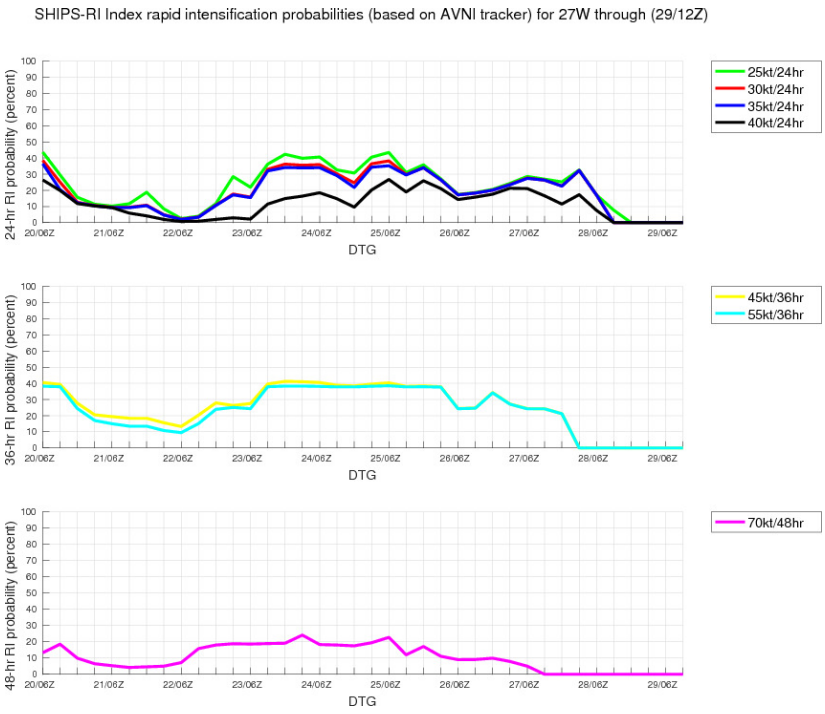

Figure 17*. Example graphic for TC 27W (2017) showing changes in SHIPS-RI rapid intensification probabilities for the listed thresholds and timeframes. Although these data significantly aid short-range predictions of rapid intensity change, additional methods to forecast the timing and extent of rapid intensity change with greater specificity and to identify the potential for extreme events are still needed.*

Many forecast challenges can be addressed using improved remotely-sensed observations and derived parameters such as atmospheric motion vectors. These data often have high spatial and temporal resolution and can be ingested into high-resolution ensemble prediction systems. The use of

coupled statistical-dynamical approaches can also help in improving the accuracy of TC predictions, especially in terms of intensity. However, despite these developments, such tools are not necessarily available to all meteorological forecast centers. Improved availability and understanding of these tools is necessary to improve their use by operational forecasters in all tropical basins.

The landfall of TCs continues to be one of the most challenging and important practical forecast problems. Work has continued to focus on (a) the structural evolution of TCs that can lead to enhanced or diminished rainfall during landfall, (b) how the environment interacts with the TC vortex, and (c) changes in the properties (friction, topography, soil moisture, etc.) of the underlying surface. Much more work is needed on all these aspects to improve forecasts of TC intensity and precipitation during landfall.

10. Acronyms and other terminology

CWB	Central Weather Bureau (Taiwan)
ECMWF	European Centre for Medium-range Weather Forecasts
EFC	eddy flux convergence
ENP	eastern North Pacific
ET	extratropical transition
JTWC	Joint Typhoon Warning Center
kt	knots; 1 knot = 1 nm per hour = 1.852 km per hour = 0.5144 m s^{-1}
LEO	low earth orbit
MAE	mean absolute error
MPI	maximum potential intensity
NATL	North Atlantic
NHC	National Hurricane Center
NWP	Numerical Weather Prediction
PV	potential vorticity
RD	rapid decay
RI	rapid intensification
RSMC	Regional Specialized Meteorological Center
SWIO	southwest Indian Ocean
TWRF	Typhoon Weather Research and Forecasting model
WNP	western North Pacific
WRF	Weather Research and Forecasting model

11. References

Bao, X. W., N. E. Davidson, H. Yu, M. C. N. Hankinson, Z. Sun, L, J. Rikus, J. Y. Liu, Z. F. Yu, and D. Wu, 2015: Diagnostics for an extreme rain event near Shanghai during the landfall of Typhoon Fitow (2013). *Mon. Wea. Rev.*, **143**, 3377-3405.

Barbary, D., O. Bousquet, and M.D. Leroux, 2017: The orographic effect of Réunion island on tropical cyclone track and intensity. *In prep. for Atmos. Sci. Lett.*

Bousquet O., D. Barbary, S. Bielli, G. Faure, T. Montmerle, and P. Brousseau, 2018: AROME-IO: A New Tool for High Resolution Modeling of Tropical Cyclones in the SW Indian Ocean. *Submitted to Quart. J. Roy. Meteor. Soc.*

Chavas, D. R., and K. A. Emanuel, 2010: A QuikSCAT climatology of tropical cyclone size. *Geophys. Res. Lett.*, **37**, L18816, doi:10.1029/2010GL044558.

Chen, D.-S. , L.-F. Hsiao, T.-C. Yeh, C.-T. Cheng, C.-T. Fong, and J.-S. Hong, 2017: Impact of the TWRF Model Resolutions on Tropical Cyclones Track, Intensity and Rainfall Predictions over the Western North Pacific. *Asia Oceania Geosciences Society (AOGS) 14th Annual Meeting*, 6-12 August, 2017, Singapore, AS17-D3-PM1, p221.

Colomb, A., T. Kriat, and M.D. Leroux, 2017. The Rapid Weakening of Very Severe Tropical Cyclone Hellen (2014). *In prep. for J. Atmos. Sci.*

DeMaria, M., and J. Kaplan, 1994: A Statistical Hurricane Intensity Prediction Scheme (SHIPS) for the Atlantic Basin. *Wea. Forecasting*, **9**, 209–220.

DeMaria, M., C.R. Sampson, J.A. Knaff, and K.D. Musgrave, 2014: Is Tropical Cyclone Intensity Guidance Improving? *Bull. Amer. Met. Soc.*, **95**, 387-398.

Deng, D., N.E. Davidson, L. Hu, K.J. Tory, M.C. Hankinson, and S. Gao, 2017: Potential vorticity perspective of vortex structure changes of tropical cyclone Bilis (2006) during a heavy rain event following landfall. *Mon. Wea. Rev*., **145**, 1875-1895.

Doyle, J. D., Y. Jin, R.M. Hodur, S. Chen, H. Jin J. Moskaitis, A. Reinecke, P. Black, J. Cummings, E. Hendricks, T. Holt, C.-S. Liou, M. Peng, C. Reynolds, K. Sashegyi, J. Schmidt, and S. Wang, 2012: Real-time tropical cyclone prediction using COAMPS-TC. *Advances in Geosci.*, **28**, 15-28, doi: 10.1142/9789814405683_0002.

Dupont, T., M. Plu, P. Caroff, and G. Faure, 2011: Verification of ensemble-based uncertainty circles around tropical cyclone track forecasts. *Wea. Forecasting*, **26**, 664–676.

Gao, S., and L. S. Chiu, 2012: Development of statistical typhoon intensity prediction: Application to satellite observed surface evaporation and rain rate (STIPER). *Wea. Forecasting*, **27**, 240–250.

Gao, S., W. Zhang, J. Liu, I.-I. Lin, L. S. Chiu, and K. Cao, 2016: Improvements in Typhoon Intensity Change Classification by Incorporating an Ocean Coupling Potential Intensity Index into Decision Trees. *Wea. Forecasting*, **31**, 95–106.

Goerss, J.S. and C.R. Sampson, 2014: Prediction of consensus tropical cyclone intensity forecast error. *Wea. Forecasting*, **29**, 750–762.

Hawkins, J., D.C. Herndon, and C.S. Velden, 2016: SSMIS tropical cyclone monitoring opportunities**.** Preprints, *32nd Conference on Hurricanes and Tropical Meteorology*, San Juan, PR, Amer. Meteor. Soc.

Herndon, D. and C.S. Velden, 2016: Estimation of tropical cyclone intensity using the CIMSS ATMS tropical cyclone intensity algorithm. *21st Conference on Satellite Meteorology, Oceanography, and Climatology*, Madison, WI, Amer. Meteor. Soc.

Hong, J.-S., C.-T. Fong, L.-F. Hsiao, Y.-C. Yu, and C.-Y. Tzeng, 2015: Ensemble typhoon quantitative precipitation forecasts model in Taiwan. *Wea. Forecasting*, **30**, 217-237.

Hsiao, L. F., D.-S. Chen, Y.-H. Kuo, Y.-R. Guo, T.-C. Yeh, J.-S. Hong, C.-T. Fong, and C.-S. Lee, 2012: Application of WRF 3DVAR to operational typhoon prediction in Taiwan: impact of outer loop and partial cycling approaches. *Wea. Forecasting*, **27**, 1249-1263.

Hsiao, L. F., X.-Y. Huang, Y.-H. Kuo, D.-S. Chen, H. Wang, C.-C. Tsai, T.-C. Yeh, J.-S. Hong, C.-T. Fong, C.-S. Lee, 2015: Blending of Global and Regional Analyses with a Spatial Filter: Application to Typhoon Prediction over the Western North Pacific Ocean. *Wea. Forecasting*, **30**, 754-770.

Huang, C.-Y., C.-A. Chen, S.-H. Chen, and D. S. Nolan, 2016: On the Upstream Track Deflection of Tropical Cyclones Past a Mountain Range: Idealized Experiments. *J. Atmos. Sci*. **73**, 3157-3180.

Kaplan, J., M. DeMaria, and J. A. Knaff, 2010: A revised tropical cyclone rapid intensification index for the Atlantic and Eastern North Pacific basins. *Wea. Forecasting*, **25**, 220–241.

Kieper, M. and H. Jiang, 2012: Predicting tropical cyclone rapid intensification using the 37 GHz ring pattern identified from passive microwave measurements. *Geophys. Res. Lett*., **39**, L13804.

Knaff, J. A., C. R. Sampson, and M. DeMaria, 2005: An operational Statistical Typhoon Intensity Prediction Scheme for the western North Pacific. *Wea. Forecasting*, **20**, 688–699.

Knaff, J. A., C. J. Slocum, K. D. Musgrave, C. R. Sampson, and B. R. Strahl, 2016: Using routinely available information to estimate tropical cyclone wind structure. *Mon. Wea. Rev.*, **144**, 1233-1247.

Kosiba, K., J. Wurman, F. J. Masters, and P. Robinson, 2013: Mapping of Near-Surface Winds in Hurricane Rita Using Finescale Radar, Anemometer, and Land-Use Data. *Mon. Wea. Rev.*, **141**, 4337-4349.

Kosiba, K. and J. Wurman, 2014: Finescale Dual-Doppler Analysis of Hurricane Boundary Layer Structures in Hurricane Frances (2004) at Landfall. *Mon. Wea. Rev.,* **142**, 1874-1891.

Leroux, M.-D., J. Meister, D. Mekies, and P. Caroff, 2017: A Climatology of Southwest Indian Ocean Tropical Systems: their Number, Tracks, Impacts, Sizes, Empirical Maximum Potential Intensity and Intensity Changes. *Accepted by J. Appl. Meteor. Climatol*.

Liang, J., and L. Wu, 2015: Sudden track changes of tropical cyclones in monsoon gyres: Full-physics, idealized numerical experiments. *J. Atmos. Sci.*, **72**, 1307-1322.

Liang, J., L. Wu, G. Gu, and Q. Liu, 2016: Rapid weakening of Typhoon Chan-Hom (2015) in a monsoon gyre. J. Geophys. Res. Atmos., **121**, 9508-9520, doi: 10.1002/2016JD025214.

Liang, J., L. Wu, and G. Gu, 2017a: A numerical study of influences of a monsoon gyre on intensity changes of Typhoon Chan-Hom (2015), *Advances in Atmospheric Sciences*, accepted.

Liang, J., L. Wu, and G. Gu, 2017b: Rapid Weakening of Tropical Cyclones in Monsoon Gyres over the Tropical Western North Pacific. *J. Climate*, accepted.

Lin, Y.-L., S.-H. Chen, and L. Liu, 2016: Orographic Influence on Basic Flow and Cyclone Circulation and Their Impacts on Track Deflection of an Idealized Tropical Cyclone. *J. Atmos. Sci.,* **73**, 3951-3974.

Milrad, S. M., E. H. Atallah, and J. R. Gyakum, 2013: Precipitation modulation by the Saint Lawrence River valley in association with transitioning tropical cyclones. *Wea. Forecasting*, **28**, 331–352.

Moore, B. J., L. F. Bosart, D. Keyser, and M. L. Jurewicz, 2013: Synoptic-Scale Environments of Predecessor Rain Events Occurring East of the Rocky Mountains in Association with Atlantic Basin Tropical Cyclones. *Mon. Wea. Rev.*, **141**, 1022–1047.

Olander, T. L. and C. S. Velden, 2007: The Advanced Dvorak Technique: Continued development of an objective scheme to estimate tropical cyclone intensity using geostationary infrared satellite imagery. *Wea. Forecasting*, **22**, 287-298.

Onderlinde, M. J., and D. S. Nolan, 2017: The tropical cyclone response to changing wind shear using the method of time-varying point-downscaling. *Journal of Advances in Modeling Earth Systems*, doi:10.1002/2016MS000796.

Peirano, C. M., K. L. Corbosiero, and B. H. Tang, 2016: Revisiting trough interactions and tropical cyclone intensity change. *Geophys. Res. Lett.*, **43**, 5509–5515.

Qin, N., D.-L. Zhang, and Y. Li, 2016: A statistical analysis of steady eyewall sizes associated with rapidly intensifying hurricanes. *Wea. Forecasting*, **31**, 737-742.

Quetelard, H. M., F. D. Bonnardot, G. D. Jumaux, and M. Bessafi, 2018. Probabilistic forecasts of tropical cyclone track and intensity through ensemble techniques. *In prep. for Quart. J. Roy. Meteor. Soc.*

Riemer, M., M. T. Montgomery, and M. E. Nicholls, 2010: A new paradigm for intensity modification of tropical cyclones: Thermodynamic impact of vertical wind shear on the inflow layer. *Atmos. Chem. Phys.*, **10**, 3163-3188.

Riemer, M., and F. Laliberté, 2015: Secondary Circulation of Tropical Cyclones in Vertical Wind Shear: Lagrangian Diagnostic and Pathways of Environmental Interaction. *J. Atmos. Sci.*, **72**, 3517-3536.

Sampson, C.R. and J.A. Knaff, 2015: A consensus forecast for tropical cyclone gale wind radii. *Wea. Forecasting*, **30**, 1397-1403.

Schmit, T.J., P. Griffith, M.M. Gunshor, J.M. Daniels, S.J. Goodman, and W.J. Lebair, 2017: A Closer Look at the ABI on the GOES-R Series. *Bull. Amer. Met. Soc.*, **98**, 681-698.

Tang, C. K., and J. C. L. Chan, 2014: Idealized simulations of the effect of local and remote topographies on tropical cyclone tracks. *Q. J. Royal Meteorol. Soc.*, **141**, 2045-2056.

Tang, C. K., and J. C. L. Chan, 2015: Idealized simulations of the effect of Taiwan topography on the tracks of tropical cyclones with different sizes. *Q. J. Royal Meteorol. Soc.*, **142**, 793-804.

Tang, C. K., and J. C. L. Chan, 2016: Idealized simulations of the effect of Taiwan topography on the tracks of tropical cyclones with different steering flow strengths, *Q. J. Royal Meteorol. Soc.*, **142**, 3211-3221.

Tsai, H.-C., and R. L. Elsberry, 2014: Applications of situation-dependent intensity and intensity spread predictions based on a weighted analog technique. *Asia-Pacific J. Atmos. Sci*., **50**, 507-518.

Tsai, H.-C., and R. L. Elsberry, 2015: Seven-day intensity and intensity spread predictions for western North Pacific tropical cyclones. *Asia-Pacific J. Atmos. Sci*., **51**, 331-342.

Tsai, H.-C., and R. L. Elsberry, 2016: Skill of western North Pacific tropical cyclone intensity forecast guidance relative to weighted-analog technique. *Asia-Pacific J. Atmos. Sci*., **52**, 281-290

Tsai, H.-C., and R. L. Elsberry, 2017: Seven-day intensity and intensity spread predictions for Atlantic tropical cyclones. *Wea. Forecasting*, **32**, 141-147.

Velden, C. S., D. C. Herndon, J. P. Kossin, J. D. Hawkins and M. DeMaria, 2006: Consensus estimates of tropical cyclone intensity using integrated multispectral (IR and MW) satellite observations. *Preprints, 27th Conference on Hurricanes and Tropical Meteorology*, Monterey, CA, Amer. Meteor. Soc.

Wang, Y., Y. Wang, and H. Fudeyasu, 2009: The Role of Typhoon Songda (2004) in Producing Distantly Located Heavy Rainfall in Japan. *Mon. Wea. Rev.*, **137**, 3699-3716.

Wang, C., and Z. Zeng, 2017: Influence of model horizontal resolution on the intensity and structure of Rammasun. *Accepted by J. Trop. Met*.

Wood, K. M., and E. A. Ritchie, 2015: A definition for rapid weakening in the North Atlantic and eastern North Pacific. *Geophys. Res. Lett.*, **42**, 10091-10097.

Wu, C.-C., T.-H. Li, and Y.-H. Huang, 2015: Influence of Mesoscale Topography on Tropical Cyclone Tracks: Further Examination of the Channeling Effect. *J. Atmos. Sci.*, **72**, 3032-3050.

Xu, J., and Y. Wang, 2015: A Statistical Analysis on the Dependence of Tropical Cyclone Intensification Rate on the Storm Intensity and Size in the North Atlantic. *Wea. Forecasting*, **30**, 692–701.

Yu, Z., Y. Wang, H. Xu, N. E. Davidson, Y. Chen, Y. Chen, and H. Yu, 2017: On the Relationship between Intensity and Rainfall Distribution in Tropical Cyclones Making Landfall over China. *J. Appl. Met. Clim.*, **56**, 2883–2901.

Zeng, Z.-H., Y. Wang, and C.-C. Wu, 2007: Environmental dynamical control of tropical cyclone intensity: An observational study. *Mon. Wea. Rev.*, **135**, 38–59.

Zhang, F., Z. Pu, and C. Wang, 2017: Effects of Boundary Layer Vertical Mixing on the Evolution of Hurricanes over Land. *Mon. Wea. Rev.,* **145,** 2343-2361.